

Anna Andersson,^a Mourad Harir,^{bc} Michael Gonsior,^d Norbert Hertkorn,^b
Philippe Schmitt-Kopplin,^{bc} Henrik Kylin,^{ae} Susanne Karlsson,^a
Muhammad Jamshaid Ashiq,^a Elin Lavonen,^f Kerstin Nilsson,^g Ämma Pettersson,^h
Helena Stavklintⁱ and David Bastviken^a

Reactions between chemical disinfectants and natural organic matter (NOM) upon drinking water treatment result in formation of potentially harmful disinfection by-products (DBPs). The diversity of DBPs formed is high and a large portion remains unknown. Previous studies have shown that non-volatile DBPs are important, as much of the total toxicity from DBPs has been related to this fraction. To further understand the composition and variation of DBPs associated with this fraction, non-target analysis with ultrahigh resolution Fourier transform ion cyclotron resonance mass spectrometry (FT-ICR MS) was employed to detect DBPs at four Swedish waterworks using different types of raw water and treatments. Samples were collected five times covering a full year. A common group of DBPs formed at all four waterworks was detected, suggesting a similar pool of DBP precursors in all raw waters that might be related to phenolic moieties. However, the largest proportion (64–92%) of the assigned chlorinated and brominated molecular formulae were unique, *i.e.* were solely found in one of the four waterworks. In contrast, the compositional variations of NOM in the raw waters and samples collected prior to chemical disinfection were rather limited. This indicated that waterworks-specific DBPs presumably originated from matrix effects at the point of disinfection, primarily explained by differences in bromide levels, disinfectants (chlorine *versus* chloramine) and different relative abundances of isomers among the NOM compositions studied. The large variation of observed DBPs in the toxicologically relevant non-volatile fraction indicates that non-targeted monitoring strategies might be valuable to ensure relevant DBP monitoring in the future.

rsc.li/es-water

A large fraction of the disinfection by-products (DBPs) formed upon drinking water treatment is unknown on a molecular level and not accounted for through current monitoring. Non-target DBP analyses employed here demonstrate that the largest portion of DBPs formed at four Swedish waterworks were unique for each plant, highlighting a large variation in the formation of non-monitored, toxicologically relevant DBPs.

Chemical disinfection constitutes an important drinking water treatment to inactivate pathogens and limit microbial

regrowth in the distribution network and prevent spread of waterborne diseases worldwide. However, the use of disinfectants, such as chlorine, chloramine, chlorine dioxide and ozone leads to the formation of disinfection by-products

† Electronic supplementary information (ESI) available: Showing figures including (i) diagrams further describing the characteristics of DBP molecular formulae formed at the four waterworks, (ii) diagrams further describing the characteristics of DBP molecular formulae that were unique and shared between the four waterworks, and (iii) Venn diagrams showing CHO and DBP compositions for each of the five sampling events separately, and tables, (iv) a list of DBP molecular formulae formed at the four waterworks, (v), a list of unique and shared DBPs formulae, and (vi) a summarized comparison of DBP formulae found in the present and in previous studies. See DOI: 10.1039/c9ew00034h

The diversity of DBPs formed makes effective monitoring challenging.^{1,11} Typically, only the regulated DBPs are monitored, *e.g.* THM4 and HAA5, which implies very limited information of the overall DBP exposure. Furthermore, consideration of differences in toxicity among the DBPs formed is critical for a relevant DBP assessment. Bioluminescence inhibition assays indicate that DBPs in the non-purgeable fraction (in the specific study defined as the total amount of adsorbed organic halogens (AOX) present after purging the sample with nitrogen for 30 minutes) are of higher toxicological relevance than DBPs in the purgeable fraction.¹² In the same study, AOX and a range of known DBPs were analysed. Most of the AOX in the purgeable fraction, *i.e.* semi- to highly volatile compounds, could be explained by known DBPs, while less than 16% could be explained in the non-purgeable fraction, *i.e.* non-volatile to semi volatile compounds, demonstrating the lack of available information of DBPs in this pool.¹² Recent work summarizing the challenges and opportunities within DBP research points towards the need of finding the key “toxicity drivers” that can explain the observed risk for bladder cancer, so that efforts to minimize exposure focus on the relevant targets.¹³ A number of studies have been carried out to analyze the non-volatile fraction of DBPs using non-target approaches, where some have focused on lab experiments,^{14–18} and a few on real waterworks.^{19–21} Previous studies indicate that there is variation and overlap of non-volatile DBPs formed at different waterworks.^{19–21} However, sampling in those studies was restricted to a single occasion, and the degree of similarity or variability between water treatment plants and treatment methods remains inconclusive. Expanding the knowledge about compositional variability of non-volatile DBPs is important to link DBP formation to water treatment conditions and evaluating remaining toxicity caused by DBPs. This study was undertaken to investigate the formation of non-volatile DBPs, covering a full seasonal cycle in four different waterworks, using different raw water sources, combinations of treatment steps, and disinfectants.

Table 1 presents basic water characteristics relevant to the DBP formation process at the four waterworks. pH was measured at room temperature within six hours after sampling, dissolved organic carbon (DOC) was measured using the non-purgeable organic carbon (NPOC) method at the accredited lab associated with each treatment plant and total chlorine

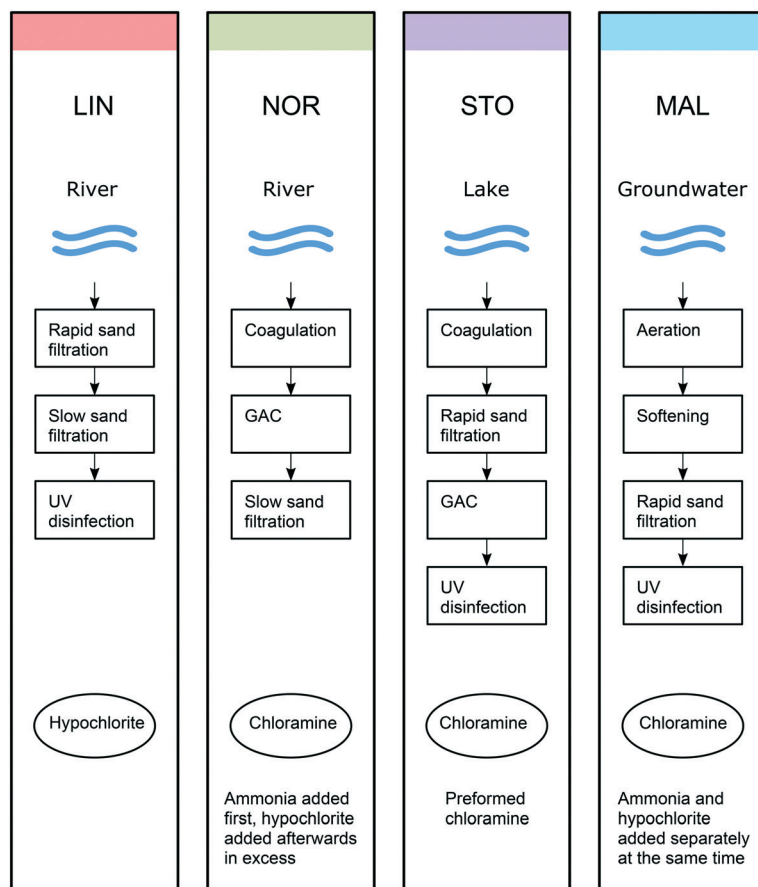


Fig. 1 Scheme of the raw water types, treatment steps and disinfectants used at the four waterworks (LIN, NOR, STO and MAL). The colours used are consistent with those used in the Venn diagrams.

Table 1 Water characteristics in the studied waterworks. Temperature, pH and total chlorine residual (mg L^{-1} as Cl_2) were measured after and DOC right before chlorine/chloramine addition. See text and Fig. 1 for descriptions of the waterworks and for explanations of their abbreviated names

Waterworks	LIN					NOR					STO					MAL				
Year	2016	2016	2016	2016	2017	2016	2016	2016	2016	2016	2017	2016	2016	2016	2016	2016	2016	2016	2016	2017
Month	Mar	May	Aug	Nov	Jan	Mar	May	Aug	Nov	Jan	Mar	May	Aug	Nov	Jan	Mar	May	Aug	Nov	Jan
Temp ($^{\circ}\text{C}$)	1.9	13.3	22.8	3.6	1.4	3.3	11.6	18.0	5.0	1.4	5.4	7.2	10.7	8.5	2.0	9.5	10.6	11.1	9.9	9.3
pH	8.3	8.3	8.2	8.3	8.2	8.5	8.5	8.0	8.2	8.3	7.0	6.7	6.8	6.9	6.8	8.2	8.1	8.3	8.2	8.1
DOC (mg L^{-1})	1.7	2.0	1.6	2.2	1.9	2.3	2.9	2.9	2.9	2.8	4.3	4.2	4.6	4.2	4.1	2.4	2.3	2.3	2.4	2.2
Total Cl_2 (mg L^{-1})	0.26	0.27	0.44	0.26	0.22	0.32	0.27	0.29	0.38	0.31	0.21	0.26	0.29	0.34	0.19	0.26	0.27	0.26	0.27	0.29

(as Cl_2) was measured on-line. Temperatures fluctuated more in LIN and NOR, compared to STO and were almost constant in MAL. pH was 8.0–8.5 at the point of disinfection at all waterworks except STO, where pH was 6.7–7.0. At STO, pH was raised to 8.0–8.5 before water was distributed. Total chlorine residual levels peaked in August for LIN and in November for NOR and STO, respectively. At MAL, all parameters measured were relatively constant throughout the year.

2.3 Sampling and solid phase extraction

Duplicate samples from the four waterworks, including raw water and water before and after chlorination/chloramination, were collected at five occasions throughout one year; in March, May, August, and November 2016, and January 2017 (months are abbreviated Mar, May, Aug, Nov and Jan, in figures and tables). The water samples (5 L) were collected in amber glass bottles and filtered immediately after sampling (GF/F, pore size $0.7 \mu\text{m}$, Whatman) into another



This journal is © The Royal Society of Chemistry 2019

diagrams visualize molar ratios of hydrogen to carbon (H/C) plotted against those of oxygen to carbon (O/C), which provides information about the degree of saturation and oxygenation (which relates to oxidation) for each assigned molecular formula. Plotting H/C ratios against mass complements common van Krevelen diagrams by showing the mass distribution as well. Kendrick mass defect (KMD) is used to organize the molecular formulae in homologous series, in which formulae are related through differences in molecular entities such as, CH₂, CHOO, C₂H₂ and H₂.³³ In this study, the homologous series were created based on CH₂, which means that compounds that have the same number of double bond equivalents (DBE, which may represent rings and double bonds) and heteroatoms (limited to oxygen in this case), but different numbers of CH₂ entities, will have the same Kendrick mass defect. The parameter *z*-score (*z*^{*}) is another independent parameter that describes homologous series³⁴ and the combined KMD and *z*^{*} diagram was used to create a modified diagram, $-KMD/z^*$ plotted against mass.³¹ This diagram shows differences in counts of CH₂ along the *x*-axis, nominal exchange of CH₄ against O along the *y*-axis and nominal exchange of CH₄ against H₂ along diagonals. For further characterization of DBPs, various indices were computed, describing double bond equivalence (DBE), aromaticity index (AI_{mod}), and average oxidation state of carbon (C_{OS}). DBE and AI_{mod} were computed according to Koch and Dittmar (2006)²⁹ and C_{OS} was calculated as eqn (1) where *n*H is the number of hydrogen atoms (neutral form), and *n*O, *n*Cl, *n*Br and *n*C are the counts of oxygen, chlorine, bromine and carbon atoms, respectively.

$$C_{OS} = -\frac{(nH \times 1) + (nO \times (-2)) + (nCl \times (-1)) + (nBr \times (-1))}{nC} \quad (1)$$

Data processing was focused on the presence or absence of individual verified DBP formulae, disregarding differences in relative intensities. With the purpose of analyzing the compositional variation of DBPs formed at the four waterworks in a clear visual way, series of Venn diagrams were created by performing multiple comparisons of individual DBPs formed at each plant. Comparisons were made 1) for each sampling month separately and 2), through combining all DBPs formed throughout the five sampling events. For comparisons between the four waterworks, 15 segments built up the Venn diagram, including both unique and shared DBPs. The data processing was performed in Matlab 2017 using the assigned elemental formula as the variable for sorting. Among duplicate FT-ICR MS spectra from each extract, there were some variability in the amount of organic material injected, leading to variability regarding if the lowest intensity peaks reached above the threshold used as detection limit. Hence, we observed some variability among duplicates in the number of detected and verified DBPs, caused by the low relative intensity of many of the alternative stable isotopic composition peaks used for verification. Overall, this verification method also underestimated the number of DBPs detected because the verification peaks in many cases

could not reach the specified detection limit. Hence, and due to the severity of this verification approach, all peaks that could be verified were accepted, and as a consequence the duplicate yielding the spectra with highest intensities were used. Relative mass peak intensities were not used in the data analysis, except to compute weighted average values of elemental compositions and indices. However, relative mass peak intensities were considered indirectly through the isotope verification filter.

3. Results and discussion

3.1 DBP composition

Table 2 presents the number of total and verified DBP molecular formulae together with average elemental compositions, elemental ratios, and various index values (all weighted against relative abundance) of verified DBPs formed at the four waterworks throughout the five sampling events. The verification process reduced the number of DBPs to 25–35% of the total number of halogenated CHO formulae found (Table 2). A large fraction of the non-verified halogenated compounds was positioned along with and in the outer range of the verified DBPs in the van Krevelen diagram, and likely had too low intensity for the alternative isotope to be found. Another group of potential DBP signatures among the non-verified DBPs was characterized by a high mass and few oxygen atoms and were found both before and after disinfection.

A summary of the verified DBP types formed at the four waterworks is shown in Fig. 2. A full list of the verified DBP formulae is provided in the ESI† (Table S1). DBPs show profound differences between the waterworks, which is also reflected in the relative abundance of chlorine and bromine containing molecular compositions among verified DBPs (Table 2). Primarily, CHO molecular compositions with one chlorine, referred to as CHOC_l formulae, were formed in LIN,

Table 2 Average values, with recognition of relative abundance, of verified DBPs (both chlorinated and brominated CHO molecular formulae selected based on criteria described in section 2.5.1) in neutral form (the mass of a proton added) computed from negative electrospray (ESI) 12 T FT-ICR mass spectra

Number of filtered formulae found	LIN	NOR	STO	MAL
<i>n</i> of total Cl [−] and Br [−] CHO formulae	1050	1297	833	823
<i>n</i> of verified Cl [−] and Br [−] CHO formulae	273	453	206	279
Characteristics of verified DBPs				
Average H [%]	40.5	40.1	41.6	39.9
Average C [%]	37.0	37.8	37.5	39.2
Average O [%]	19.7	19.3	18.2	18.5
Average Cl [%]	2.7	2.7	2.4	0.3
Average Br [%]	0.0	0.1	0.3	2.2
Computed average H/C ratio	1.09	1.06	1.11	1.02
Computed average O/C ratio	0.53	0.51	0.48	0.47
Computed average C/Cl ratio	13.7	13.8	15.5	147
Computed average C/Br ratio	1126	564	130	18.1
Average carbon oxidation state (C _{OS})	0.070	0.048	−0.056	0.008
Average DBE	7.57	7.74	7.44	8.58
Average DBE/C	0.48	0.50	0.47	0.52
Average AI _{mod}	0.35	0.38	0.36	0.42
Mass weighted average [Da]	383.0	372.9	373.8	415.4



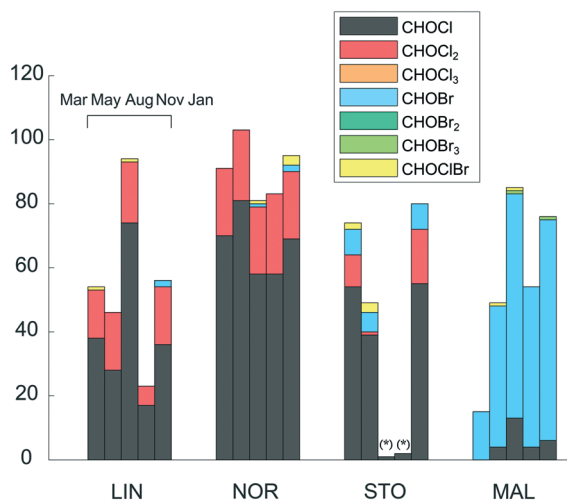


Fig. 2 Bar plot showing the number and type of verified DBP formulae formed at the four waterworks. (*) few DBPs were verified for STO in Aug and Nov due to general low spectral intensities for those samples (see text).

NOR and STO, whereas CHO molecular compositions with one bromine, referred to as CHOBBr formulae, were abundant in MAL. DBPs with two chlorine atoms were consistently formed in LIN and NOR, while few such components were found in the other plants. Tentatively, this could be related to disinfectant type since both LIN and NOR waters were exposed to free chlorine, which is a more effective halogenation agent compared to chloramine, facilitating the incorporation of multiple chlorine atoms. In previous DBP studies based on FT-ICR MS, CHOCI_2 molecular formulae were frequently found at waterworks using NaOCl disinfection and not at those using chloramine, supporting this interpretation.^{19–21}

Overall, few CHOCI_3 molecular formulae were found, even at LIN and NOR. For activated aromatic structures, such as phenolic compounds, that undergo electrophilic aromatic substitution reactions, the chlorination reaction rate decreases after each chlorine incorporation, which means that the conditions required for chlorine incorporation change during the continuous chlorination.³⁵ This may explain the low number of CHOCI_3 molecular formulae found. Possibly, CHOCI_3 molecular formulae did form, but were further transformed to end-DBPs, such as THMs, through rapid hydrolysis reactions (more specifically referred to as the haloform reaction), and were no longer amenable for FT-ICR MS detection (due to losses of volatile compounds during sample preparation and because of their low molecular weight). Previous chlorination experiments on isolated NOM fractions prior to FT-ICR MS detection, showed that a fraction constituting oxygenated, unsaturated compounds was the only fraction producing DBPs with multiple chlorine atoms, indicating that these differences also are linked to NOM characteristics.^{14,36} When comparing those CHOCI_2 formulae with the CHOCI_2 formulae found in this study, 12 of 65 DBP formulae were common, indicating that part of the CHOCI_2 formulae detected in this study was formed through reaction with similar precursors.¹⁴

The bromide concentration in the raw water at MAL was 0.28 mg L^{-1} , *i.e.* substantially higher compared to the other waterworks, explaining the formation of elevated levels of brominated DBPs there. In this case, bromide probably entered the groundwater from the old marine sediments dominating the region.³⁷ It is evident that the presence of bromide in the MAL water drives the formation towards brominated DBPs while minimizing the formation of chlorinated DBPs. This may be explained by the greater reaction rate constant of NH_2Br , NHBr_2 and NHClBr (which are formed through reactions between NH_2Cl and Br^-) to form Br-DBPs, compared to the reaction rate between NH_2Cl and NOM to form Cl-DBPs, assuming slow reaction sites,³⁸ which are estimated to be the major reaction sites for Br-DBP formation and about 50% of Cl-DBP formation upon chloramination.³⁹ To further explain the concept of fast and slow reaction sites, halogen oxidants have been found to follow an initial rapid consumption phase, in which *e.g.* aromatic, phenolic compounds (fast reaction sites) react, followed by a slower consumption phase where NOM with *e.g.* electron withdrawing functional groups, such as carboxyl or carbonyl groups, (slow reaction sites) react.³⁸ Also, the low DOC level in MAL results in a relatively high Br^-/DOC ratio which also favours the reaction pathway towards brominated DBPs.⁶ CHOBBr formulae were the dominant Br-DBP type detected while few CHOBBr_2 or CHOBBr_3 formulae were found. This might be due to the lower substitution rates of the bromoamines and bromochloroamine species, compared to chlorine (HOCl/OCl^-).³⁹ In general, very few combined chlorine–bromine molecular formulae were assigned and those formulae either had high H/C and low O/C ratios, suggesting aliphatic compounds, or constituted a simple composition, $\text{C}_5\text{HO}_3\text{ClBr}_2$, which has been identified as 2,2,4-dibromochloro-5-hydroxy-4-cyclopentene-1,3-dione (HCD) in previous work.⁴⁰ The low number of verified DBPs determined for August and November in STO was caused by low mass spectral intensities of those samples, causing few DBP isotope mass peaks to be found. The low intensities were likely due to ion suppression or because of non-optimal dilution for those samples specifically. However, CHOCI and CHOBBr formulae not present before disinfection were formed in STO also in Aug and Nov, but very few were verified with their corresponding isotope mass peaks.

3.2 DBP characteristics

The majority of verified DBP compositions were observed in the mass range 300–500 Da and distributed at O/C and H/C ratios of 0.3–0.7 and 0.7–1.4, respectively (Fig. 3). DBPs from the four waterworks were overall similar in average H, C and O elemental compositions (Table 2). However, DBPs formed in MAL (mostly brominated), showed higher relative abundances of carbon and higher DBE and AI_{mod} (see section 2.5.2) compared to those found in the other plants. The latter indicated higher proportions of aromatic, unsaturated compounds among the brominated DBPs. DBPs formed in LIN showed higher average mass (Table 2), compared to those



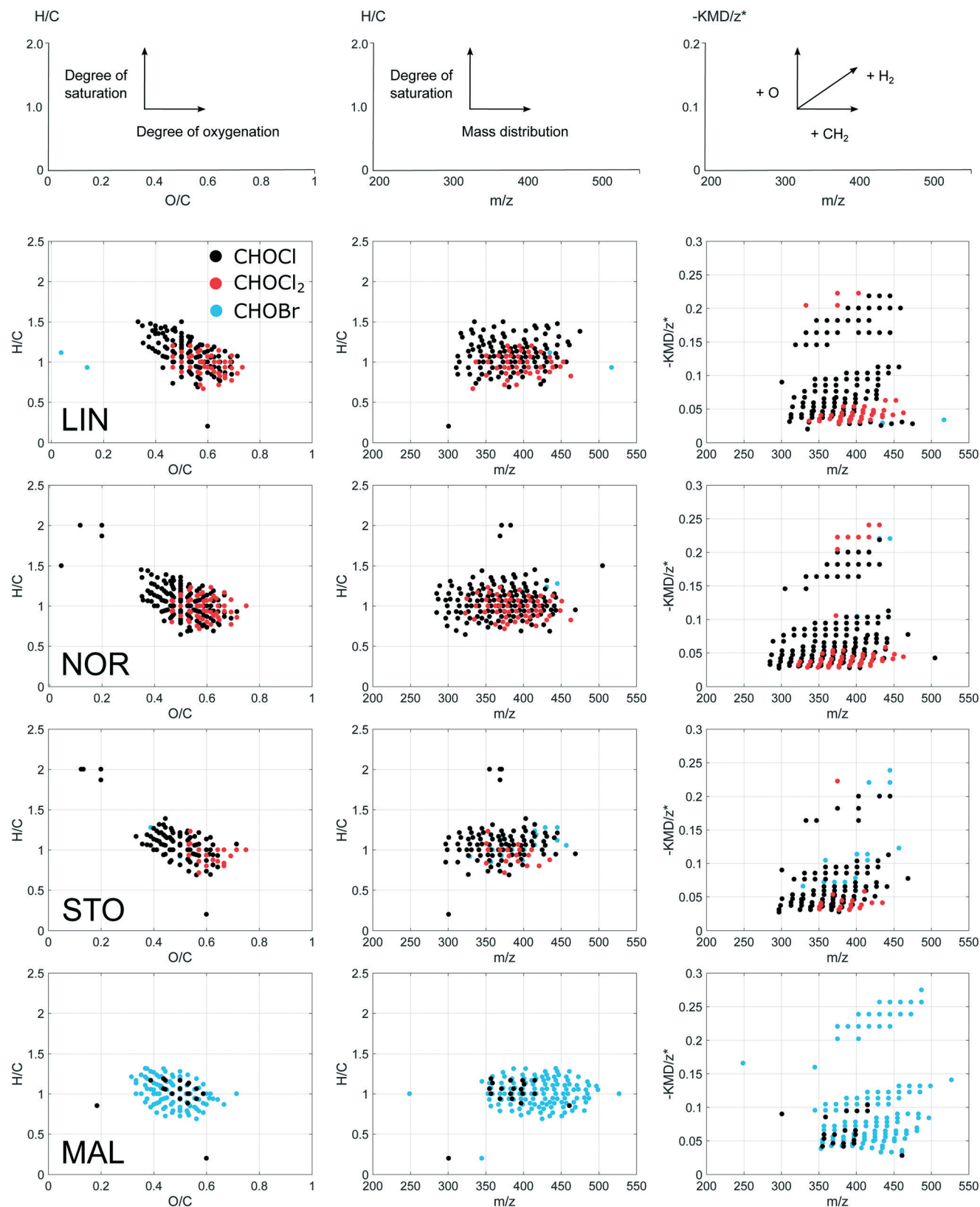


Fig. 3 Van Krevelen, H/C against mass and modified Kendrick plots for the verified DBPs formed at each waterworks (DBPs formed throughout the five sampling events combined). Plots are described in more detail in section 2.5.2.



The verified DBPs showed near congruent distributions (Fig. 3), in spite of the observed specific differences between waterworks, also when compared to previous studies.^{20,21} Based on their elemental ratios, most of the observed DBPs can be referred to as polyphenol-like compounds;^{24,32} however, FT-ICR MS is not capable of supplying structural information beyond what can be inferred from molecular formulae alone. DBPs with low H/C ratios (~ 0.7 – 0.8) indicate a deficiency in H and suggest presence of more condensed aromatic structures among these DBPs. The verified DBPs detected here typically have between 12–20 carbon atoms and 6–11 oxygen atoms, where 8 oxygen atoms is most common when combining all DBPs formed, including both chlorinated and brominated species (ESI[†] Fig. S3 and S4). When

Fig. S8–S12 in the ESI† visualize DBPs of the different segments of the Venn diagram (Fig. 4), including the unique DBPs for each treatment plant (ESI† Fig. S8 and S9) and the DBPs that were common in all four, three and two of the waterworks (ESI† Fig. S10–S12). Notably, the unique LIN DBPs appeared in a more confined chemical space, while unique NOR DBPs covered a larger area of the van Krevelen diagram, indicating a greater diversity of DBPs formed at NOR, most



Fig. 4 The Venn diagram shows the number of unique and shared verified DBPs formed at the four waterworks (DBPs formed throughout the five sampling events combined).

likely due to greater diversity of raw water NOM molecules. At both LIN and NOR, CHOC_2 formulae were part of the unique DBPs as well as shared between the two, which supports previous reasoning regarding connections of DBPs to free chlorine exposure in those plants. Interestingly, the DBPs shared between all waterworks occurred in a quite defined position in the van Krevelen diagram, suggesting these compounds were favourably formed even for different raw waters and treatments (Fig. 5). The modified Kendrick plot of these DBPs also showed a clear pattern which indicates that these compounds might be related *via* few nominal chemical transformations, including methylation/demethylation, alkyl chain elongation, and oxidation/reduction.

3.4 Do raw water NOM or treatment processes determine the DBP composition?

To investigate the origin of the DBP variation between the four plants, analogous comparisons were performed using raw water CHO molecular formulae from each water treatment plant. Interestingly, these Venn diagrams (ESI† Fig. S13) showed opposite trends, displaying a large portion of shared formulae in case of CHO compounds as opposed to DBPs (*cf.* above). For all five occasions of sample collection, 77–87% of the CHO formulae present in the raw waters were

common for two or more plants and the majority were shared between all four plants (Fig. S13†). However, it is very likely that several isomers with identical molecular composition exist in one sample, particularly among the highly numerous CHO compounds.²⁶ Consequently, it is possible that variations of the observed DBP composition arose from differences in isomeric structures of NOM and their relative abundance in the four waterworks. Therefore, DBP diversity could reflect the actual NOM molecular diversity in a more comprehensible way than the highly convoluted mass spectra of NOM itself would show.

This might apply to both raw waters (Fig. S13†) and waters right before the point of chemical disinfection where the similar pattern were observed, *i.e.* that the majority of CHO formulae were shared between all four plants (Fig. S14†). A less probable alternative is that the unique sets of pre-disinfection CHO formulae have produced the unique sets of DBPs. This hypothesis was investigated by back-calculating the respective CHO precursors from the verified DBPs formed at each plant, each month separately, assuming both substitution and addition reactions. When comparing each of the 20 Venn diagram segments of unique CHO formulae with the 20 Venn diagram segments of unique back-calculated CHO precursors (based on verified DBPs), only seven formulae of 689 matched, giving low support to this assumption. Instead, a large portion (70–100%) of the potential CHO precursors, determined from unique DBP formulae, were found among the CHO formulae shared between all four plants. Thus, it is clear that information related to structural features of NOM will be necessary to complement NOM compositional characteristics to fully understand the variation of DBPs. However, obtaining such information is beyond the scope of this study.

3.5 Comparisons with previous studies

The verified DBP formulae found in this study were also compared to those identified in previous studies, summarized in ESI† Tables S3–S5. It is important to note that two different types of SPE-cartridges have been used to extract NOM in these studies, Bond Elut PPL and Sep-Pak C18 (ESI† Tables S3 and S4). Comparative analysis of extracted Suwannee River NOM has recently demonstrated fair congruence of PPL- and

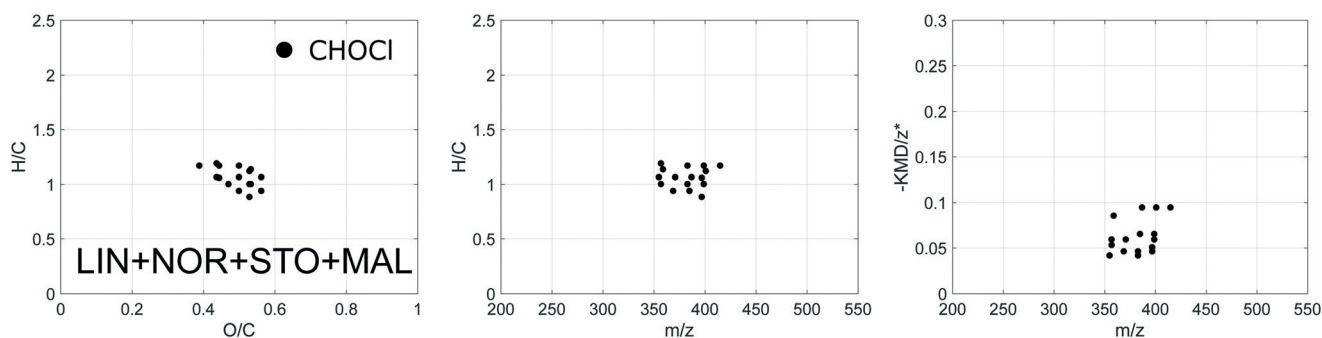


Fig. 5 Van Krevelen, H/C against mass and modified Kendrick mass plots for the verified DBPs shared between all four plants (DBPs formed throughout the five sampling events combined).



The application of high-dose formation potential experiments of Suwannee River fulvic acid in the presence of bromide (1848 DBP compositions in total) contained almost the entire set of verified DBP formulae found in this study (360 different DBPs), formed both through chlorine and chloramine disinfection.¹⁷ This is logical, because in high-dose chlorination experiments, all potential DBPs that can result from the precursor material will form due to the large excess of chlorine, and the Suwannee River may have highly diverse NOM including precursors for most possible DBPs. In the Swedish waterworks, the aim is minimum DBP production by removal of NOM in up-stream treatment processes and minimizing the dose of reactive chlorine, resulting in less DBPs being formed, compared to in high-dose experiments on the full range of NOM. Instead, local conditions are steering and limiting the DBP formation, *e.g.* through the abundance and reactivity of specific NOM structures, variations in bromide levels and disinfectant type, driving the formation of waterworks-specific DBPs.

Through non-target analysis and comparison at the molecular level, this study has brought qualitative insights into DBP

- 1 E. D. Wagner and M. J. Plewa, CHO cell cytotoxicity and genotoxicity analyses of disinfection by-products: An updated review, *J. Environ. Sci.*, 2017, 58, 64–76.
- 2 C. M. Villanueva, S. Cordier, L. Font-Ribera, L. A. Salas and P. Levallois, Overview of Disinfection By-products and Associated Health Effects, *Curr. Environ. Health Rep.*, 2015, 2, 107–115.
- 3 C. M. Villanueva, K. P. Cantor, J. O. Grimalt, N. Malats, D. Silverman, A. Tardon, R. Garcia-Closas, C. Serra, A. Carrato, G. Castaño-Vinyals, R. Marcos, N. Rothman, F. X. Real, M. Dosemeci and M. Kogevinas, Bladder Cancer and Exposure to Water Disinfection By-Products through Ingestion, Bathing, Showering, and Swimming in Pools, *Am. J. Epidemiol.*, 2007, 165, 148–156.
- 4 S. D. Richardson, M. J. Plewa, E. D. Wagner, R. Schoeny and D. M. DeMarini, Occurrence, genotoxicity, and

- carcinogenicity of regulated and emerging disinfection by-products in drinking water: a review and roadmap for research, *Mutat. Res.*, 2007, **636**, 178–242.
- 5 S. D. Richardson and T. A. Ternes, Water Analysis: Emerging Contaminants and Current Issues, *Anal. Chem.*, 2018, **90**, 398–428.
 - 6 L. Liang and P. C. Singer, Factors influencing the formation and relative distribution of haloacetic acids and trihalomethanes in drinking water, *Environ. Sci. Technol.*, 2003, **37**, 2920–2928.
 - 7 C. Postigo, P. Emiliano, D. Barceló and F. Valero, Chemical characterization and relative toxicity assessment of disinfection byproduct mixtures in a large drinking water supply network, *J. Hazard. Mater.*, 2018, **359**, 166–173.
 - 8 V. K. Sharma, R. Zboril and T. J. McDonald, Formation and toxicity of brominated disinfection byproducts during chlorination and chloramination of water: A review, *J. Environ. Sci. Health, Part B*, 2014, **49**, 212–228.
 - 9 A. A. Kampioti and E. G. Stephanou, The impact of bromide on the formation of neutral and acidic disinfection by-products (DBPs) in Mediterranean chlorinated drinking water, *Water Res.*, 2002, **36**, 2596–2606.
 - 10 C. Postigo, S. D. Richardson and D. Barceló, Formation of iodo-trihalomethanes, iodo-haloacetic acids, and halo-acetaldehydes during chlorination and chloramination of iodine containing waters in laboratory controlled reactions, *J. Environ. Sci.*, 2017, **58**, 127–134.
 - 11 S. W. Krasner, The formation and control of emerging disinfection by-products of health concern, *Philos. Trans. R. Soc., A*, 2009, **367**, 4077–4095.
 - 12 D. Stalter, L. I. Peters, E. O'Malley, J. Y. M. Tang, M. Revalor, M. J. Farré, K. Watson, U. Von Gunten and B. I. Escher, Sample Enrichment for Bioanalytical Assessment of Disinfected Drinking Water: Concentrating the Polar, the Volatiles, and the Unknowns, *Environ. Sci. Technol.*, 2016, **50**, 6495–6505.
 - 13 X. F. Li and W. A. Mitch, Drinking Water Disinfection Byproducts (DBPs) and Human Health Effects: Multidisciplinary Challenges and Opportunities, *Environ. Sci. Technol.*, 2018, **52**, 1681–1689.
 - 14 B. D. Harris, T. A. Brown, J. L. McGehee, D. Houserova, B. A. Jackson, B. C. Buchel, L. C. Krajewski, A. J. Whelton and A. C. Stenson, Characterization of Disinfection By-Products from Chromatographically Isolated NOM through High-Resolution Mass Spectrometry, *Environ. Sci. Technol.*, 2015, **49**, 14239–14248.
 - 15 H. Zhang and M. Yang, Characterization of brominated disinfection byproducts formed during chloramination of fulvic acid in the presence of bromide, *Sci. Total Environ.*, 2018, **627**, 118–124.
 - 16 H. Zhang, Y. Zhang, Q. Shi, J. Hu, M. Chu, J. Yu and M. Yang, Study on transformation of natural organic matter in source water during chlorination and its chlorinated products using ultrahigh resolution mass spectrometry, *Environ. Sci. Technol.*, 2012, **46**, 4396–4402.
 - 17 H. Zhang, Y. Zhang, Q. Shi, H. Zheng and M. Yang, Characterization of unknown brominated disinfection byproducts during chlorination using ultrahigh resolution mass spectrometry, *Environ. Sci. Technol.*, 2014, **48**, 3112–3119.
 - 18 X. Wang, J. Wang, Y. Zhang, Q. Shi, H. Zhang, Y. Zhang and M. Yang, Characterization of unknown iodinated disinfection byproducts during chlorination/chloramination using ultrahigh resolution mass spectrometry, *Sci. Total Environ.*, 2016, **554–555**, 83–88.
 - 19 H. Zhang, Y. Zhang, Q. Shi, S. Ren, J. Yu, F. Ji, W. Luo and M. Yang, Characterization of low molecular weight dissolved natural organic matter along the treatment trait of a waterworks using Fourier transform ion cyclotron resonance mass spectrometry, *Water Res.*, 2012, **46**, 5197–5204.
 - 20 M. Gonsior, P. Schmitt-Kopplin, H. Stavklint, S. D. Richardson, N. Hertkorn and D. Bastviken, Changes in Dissolved Organic Matter during the Treatment Processes of a Drinking Water Plant in Sweden and Formation of Previously Unknown Disinfection Byproducts, *Environ. Sci. Technol.*, 2014, **48**, 12714–12722.
 - 21 E. E. Lavonen, M. Gonsior, L. J. Tranvik, P. Schmitt-Kopplin and S. J. Köhler, Selective chlorination of natural organic matter: Identification of previously unknown disinfection byproducts, *Environ. Sci. Technol.*, 2013, **47**, 2264–2271.
 - 22 J. L. Luek, M. Harir, P. Schmitt-Kopplin, P. J. Mouser and M. Gonsior, Temporal dynamics of halogenated organic compounds in Marcellus Shale flowback, *Water Res.*, 2018, **136**, 200–206.
 - 23 M. Gonsior, M. Zwartjes, W. J. Cooper, W. Song, K. P. Ishida, L. Y. Tseng, M. K. Jeung, D. Rosso, N. Hertkorn and P. Schmitt-Kopplin, Molecular characterization of effluent organic matter identified by ultrahigh resolution mass spectrometry, *Water Res.*, 2011, **45**, 2943–2953.
 - 24 K. Mopper, A. Stubbins, J. D. Ritchie, H. M. Bialk and P. G. Hatcher, Advanced instrumental approaches for characterization of marine dissolved organic matter: Extraction techniques, mass spectrometry, and nuclear magnetic resonance spectroscopy, *Chem. Rev.*, 2007, **107**, 419–442.
 - 25 E. B. Kujawinski, R. Del Vecchio, N. V. Blough, G. C. Klein and A. G. Marshall, Probing molecular-level transformations of dissolved organic matter: insights on photochemical degradation and protozoan modification of DOM from electrospray ionization Fourier transform ion cyclotron resonance mass spectrometry, *Mar. Chem.*, 2004, **92**, 23–37.
 - 26 N. Hertkorn, C. Ruecker, M. Meringer, R. Gugisch, M. Frommberger, E. M. Perdue, M. Witt and P. Schmitt-Kopplin, High-precision frequency measurements: Indispensable tools at the core of the molecular-level analysis of complex systems, *Anal. Bioanal. Chem.*, 2007, **389**, 1311–1327.
 - 27 T. Dittmar, B. Koch, N. Hertkorn and G. Kattner, A simple and efficient method for the solid-phase extraction of dissolved organic matter (SPE-DOM) from seawater, *Limnol. Oceanogr.: Methods*, 2008, **6**, 230–235.
 - 28 Y. Li, M. Harir, J. Uhl, B. Kanawati, M. Lucio, K. S. Smirnov, B. P. Koch, P. Schmitt-Kopplin and N. Hertkorn, How



- representative are dissolved organic matter (DOM) extracts? A comprehensive study of sorbent selectivity for DOM isolation, *Water Res.*, 2017, **116**, 316–323.
- 29 B. P. Koch and T. Dittmar, From mass to structure: An aromaticity index for high-resolution mass data of natural organic matter, *Rapid Commun. Mass Spectrom.*, 2006, **20**, 926–932.
 - 30 E. Pretsch, P. Bühlmann and M. Badertscher, *Structure determination of organic compounds: Tables of spectral data*, Springer, Berlin Heidelberg, 2009.
 - 31 S. Shakeri Yekta, M. Gonsior, P. Schmitt-Kopplin and B. H. Svensson, Characterization of dissolved organic matter in full scale continuous stirred tank biogas reactors using ultrahigh resolution mass spectrometry: A qualitative overview, *Environ. Sci. Technol.*, 2012, **46**, 12711–12719.
 - 32 S. Kim, R. W. Kramer and P. G. Hatcher, Graphical method for analysis of ultrahigh-resolution broadband mass spectra of natural organic matter, the van Krevelen diagram, *Anal. Chem.*, 2003, **75**, 5336–5344.
 - 33 C. A. Hughey, C. L. Hendrickson, R. P. Rodgers, A. G. Marshall and K. Qian, Kendrick mass defect spectrum: A compact visual analysis for ultrahigh-resolution broadband mass spectra, *Anal. Chem.*, 2001, **73**, 4676–4681.
 - 34 A. C. Stenson, A. G. Marshall and W. T. Cooper, Exact masses and chemical formulas of individual Suwannee River fulvic acids from ultrahigh resolution electrospray ionization Fourier transform ion cyclotron resonance mass spectra, *Anal. Chem.*, 2003, **75**, 1275–1284.
 - 35 M. Deborde and U. Von Gunten, Reactions of chlorine with inorganic and organic compounds during water treatment—kinetics and mechanisms: a critical review, *Water Res.*, 2008, **42**, 13–51.
 - 36 A. C. Stenson, Reversed-phase chromatography fractionation tailored to mass spectral characterization of humic substances, *Environ. Sci. Technol.*, 2008, **42**, 2060–2065.
 - 37 Malmö-VA-verk, *Grundvattenmodell över alnarpsströmmen*, 2004.
 - 38 P. Westerhoff, P. Chao and H. Mash, Reactivity of natural organic matter with aqueous chlorine and bromine, *Water Res.*, 2004, **38**, 1502–1513.
 - 39 X. Zhu and X. Zhang, Modeling the formation of TOCl, TOBr and TOI during chlor(am)ination of drinking water, *Water Res.*, 2016, **96**, 166–176.
 - 40 H. Zhai, X. Zhang, X. Zhu, J. Liu and M. Ji, Formation of brominated disinfection byproducts during chloramination of drinking water: New polar species and overall kinetics, *Environ. Sci. Technol.*, 2014, **48**, 2579–2588.
 - 41 H. Gallard and U. von Gunten, Chlorination of phenols: Kinetics and formation of chloroform, *Environ. Sci. Technol.*, 2002, **36**, 884–890.

